


Topological transitions in a model for proximity-induced superconductivityNavketan Batra, Swagatam Nayak, and Sanjeev Kumar *Department of Physical Sciences, Indian Institute of Science Education and Research (IISER) Mohali,
Sector 81, S.A.S. Nagar, Manauli P. O. 140306, India* (Received 6 February 2019; revised manuscript received 9 December 2019; published 30 December 2019)

Using a prototype model for proximity-induced superconductivity on a bilayer square lattice, we show that interlayer tunneling can drive change in topology of the Bogoliubov quasiparticle bands. Starting with topologically trivial superconductors, transitions to a nontrivial $p_x + ip_y$ state and back to another trivial state are discovered. We characterize these phases in terms of edge-state spectra and Chern indices. We show that these transitions can also be controlled by experimentally viable control parameters, the bandwidth of the metallic layer, and the gate potential. Insights from our results on a simple model for proximity-induced superconductivity may open up a new route to discover topological superconductors.

DOI: [10.1103/PhysRevB.100.214517](https://doi.org/10.1103/PhysRevB.100.214517)**I. INTRODUCTION**

Since the early 2000s there has been a paradigm shift in the general approach to understand electronic properties of crystalline solids. Knowledge of topological character of the single particle bands turns out to be crucial for comprehending certain exotic electronic properties [1]. This change in approach originated in the discovery of topological insulators, materials that are insulating in the bulk but support topologically protected metallic surface states [2–5]. Superconductivity, a fascinating phenomenon in its own right, has intrigued physicists time and again by appearing in unexpected settings. The most recent examples are the “magic angle” superconductivity in bilayer graphene [6,7] and the tip-induced superconductivity in Cd_3As_2 [8,9]. The discovery of topological insulators motivated a similar search for materials that are superconducting (SC) in the bulk but support gapless modes on surfaces [10–14]. The key is to find ways to alter the band structure of the relevant Bogoliubov quasiparticle bands. In addition to being of fundamental interest, topological superconductors are considered as building blocks of decoherence-free quantum computers [15–20]. The existing proposals to achieve this involve (i) nanostructuring of ferromagnetic chains on surfaces of conventional superconductors [21–23] and (ii) interfaces or sandwiches between conventional superconductors and materials with strong spin-orbit coupling [24–26].

The existence of superconductivity in atomically thin layers has recently been reported by various groups. Superconductivity in a single-atomic layer film of Pb grown on Si(111) substrate was observed [27]. A monolayer of CuO_2 grown on cuprate substrate was found SC [28]. Unconventional, possibly topological, superconductivity is reported at the interface between LaAlO_3 and SrTiO_3 [29]. Proximity-induced topological superconductivity has been proposed for bilayer graphene [30]. Superconductivity can be induced, with no accompanying structural changes, in NbAs_2 by applying external pressure [31]. The tip-induced SC phase

of Cd_3As_2 has recently been stabilized in thin films [32]. These diverse material examples share a common feature—superconductivity appears when coupling between two layers is altered. Motivated by the role of proximity effect in a variety of superconductors, we explore this effect in a general setting with focus on inducing topologically nontrivial character in superconductors.

In this work, we show that simple interlayer tunneling can alter the topology of Bogoliubov quasiparticle bands. This is achieved in a prototypical model of proximity-induced superconductivity where a SC layer of square lattice is tunneling coupled to a tight-binding layer. The calculations are performed within an unrestricted mean-field approach, allowing for the existence of multiple symmetries of the SC order parameters (OPs). We find that interlayer tunneling can induce transition to topologically nontrivial state with $p_x + ip_y$ symmetry. This is qualitatively different from the existing proposals where a combination of s -wave pairing, spin-orbit coupling, and magnetic field is necessary to obtain a chiral p -wave state. A complete characterization of the band topology is carried out via Berry curvature and Chern number calculations complemented by the edge spectra in cylinder geometry. An interplay among different OP symmetries in a two-band setting is responsible for the transitions. Additionally, we find a connection between the topological transitions and the Lifshitz transitions in the underlying metallic bands. The generic nature of the model suggests that this can be applicable, with suitable variations, to a wide class of systems that invoke proximity effect [6,8,9,27–31].

II. BILAYER MODEL FOR PROXIMITY-INDUCED SUPERCONDUCTIVITY

As a prototype model for proximity-induced superconductivity, we consider an extended attractive Hubbard Hamiltonian defined on a two-dimensional square lattice coupled via interlayer tunneling to a tight-binding layer. The model is

described by the Hamiltonian,

$$\begin{aligned}
H &= H_1 + H_2 + H_{12}, \\
H_1 &= -t_1 \sum_{(ij),\sigma} [c_{i\sigma 1}^\dagger c_{j\sigma 1} + \text{H.c.}] - \mu_1 \sum_{i\sigma} c_{i\sigma 1}^\dagger c_{i\sigma 1} \\
&\quad - U \sum_i n_{i\uparrow 1} n_{i\downarrow 1} - V \sum_{(ij)} n_{i1} n_{j1}, \\
H_2 &= -t_2 \sum_{(ij),\sigma} [c_{i\sigma 2}^\dagger c_{j\sigma 2} + \text{H.c.}] - \mu_2 \sum_{i\sigma} c_{i\sigma 2}^\dagger c_{i\sigma 2}, \\
H_{12} &= -\tilde{t} \sum_{i\sigma} [c_{i\sigma 1}^\dagger c_{i\sigma 2} + \text{H.c.}]. \quad (1)
\end{aligned}$$

Here $c_{i\sigma l} (c_{i\sigma l}^\dagger)$ annihilates (creates) an electron in layer l at site i with spin σ , $\langle ij \rangle$ implies that sites i and j are nearest neighbors within a layer. μ_l is the effective layer-dependent chemical potential representing the combined effects of the thermodynamic chemical potential, on-site energies of two layers, and the applied electric field normal to the bilayer. The layer-resolved local number operators are given by $n_{i\sigma l} = c_{i\sigma l}^\dagger c_{i\sigma l}$ and $n_{il} = n_{i\uparrow l} + n_{i\downarrow l}$. $U(V)$ denotes the strength of on-site (nearest-neighbor) attractive interaction in layer 1. Using $t_1 = 1$ as the basic energy scale, and restricting ourselves to zero temperatures ($T = 0$), we are left with six independent parameters in the Hamiltonian, *viz.*, $t_2, \tilde{t}, U, V, \mu_1$, and μ_2 . In order to avoid a brute-force exploration of this large parameter space, we make use of the recently reported comprehensive phase diagram of the monolayer model [33]. We set $U = 1$ throughout the paper.

III. METHOD

We analyze the Hamiltonian in Eq. (1) by making a mean-field Bogoliubov-deGennes (BdG) approximation for the interaction term [34–36]. In the intersite attractive term we ignore the same-spin attraction parts $n_{i\uparrow} n_{j\uparrow}$ and $n_{i\downarrow} n_{j\downarrow}$ [33]. Following the standard mean-field decoupling in the pairing channel, we arrive at the pairing Hamiltonian for layer 1,

$$\begin{aligned}
H_1^{\text{BdG}} &= -t_1 \sum_{(ij),\sigma} [c_{i\sigma 1}^\dagger c_{j\sigma 1} + \text{H.c.}] - \mu_1 \sum_{i\sigma} c_{i\sigma 1}^\dagger c_{i\sigma 1} \\
&\quad - U \sum_i [\Delta_{i,1} c_{i\uparrow 1}^\dagger c_{i\downarrow 1}^\dagger + \text{H.c.}] \\
&\quad - V \sum_{i\gamma} [\Delta_{i,\gamma,1}^+ c_{i\uparrow 1}^\dagger c_{i+\gamma,1}^\dagger + \Delta_{i,\gamma,1}^- c_{i-\gamma,1}^\dagger c_{i\uparrow 1}^\dagger + \text{H.c.}] \\
&\quad + U \sum_i |\Delta_{i,1}|^2 + V \sum_{i\gamma} [|\Delta_{i,\gamma,1}^+|^2 + |\Delta_{i,\gamma,1}^-|^2]. \quad (2)
\end{aligned}$$

In the above we have introduced the pair expectation values in the ground state as $\Delta_{i,l} = \langle c_{i\downarrow l} c_{i\uparrow l} \rangle$, $\Delta_{i,\gamma,l}^+ = \langle c_{i+\gamma,1} c_{i\uparrow l} \rangle$, and $\Delta_{i,\gamma,l}^- = \langle c_{i-\gamma,1} c_{i\uparrow l} \rangle$, where γ denotes the unit vectors $+\hat{x}$ and $+\hat{y}$ on the square lattice and l is the layer index. Note that we do not impose the commonly used spin-singlet symmetry constraint on the pair expectation values. In general, $\Delta_{i,\gamma,l}^+ \neq \Delta_{i+\gamma,\gamma,l}^-$, and spin-triplet component of superconductivity is allowed to exist as a broken-symmetry mean-field phase. Indeed, it has recently been shown that a triplet SC state with $S_z = 0$ is possible in models and experiments [33,37].

Assuming translational invariance, $\Delta_{i,l} \equiv \Delta_{0,l}$ and $\Delta_{i,x/y,l}^\pm \equiv \Delta_{x/y,l}^\pm$, the Hamiltonian in \mathbf{k} -space becomes [38]

$$\begin{aligned}
H^{\text{MF}} &= \sum_{\mathbf{k}} \left(\sum_{\sigma,l} \xi_l(\mathbf{k}) c_{\mathbf{k}\sigma l}^\dagger c_{\mathbf{k}\sigma l} + [\Delta_1^{\uparrow\downarrow}(\mathbf{k}) c_{\mathbf{k}\uparrow 1}^\dagger c_{-\mathbf{k}\downarrow 1}^\dagger + \text{H.c.}] \right. \\
&\quad \left. - \tilde{t} \sum_{\sigma} [c_{\mathbf{k}\sigma 1}^\dagger c_{\mathbf{k}\sigma 2} + c_{\mathbf{k}\sigma 2}^\dagger c_{\mathbf{k}\sigma 1}] \right), \quad (3)
\end{aligned}$$

where

$$\begin{aligned}
\xi_l(\mathbf{k}) &= -2t_l (\cos k_x + \cos k_y) - \mu_l \\
\Delta_1^{\uparrow\downarrow}(\mathbf{k}) &= -U \Delta_{0,1} - V (e^{-ik_x} \Delta_{x,1}^+ + e^{ik_x} \Delta_{x,1}^- \\
&\quad + e^{-ik_y} \Delta_{y,1}^+ + e^{ik_y} \Delta_{y,1}^-). \quad (4)
\end{aligned}$$

The Hamiltonian Eq. (3) is diagonalized using bilayer-generalized Bogoliubov transformations, $c_{\mathbf{k}\sigma l} = \sum_n (u_{\mathbf{k}\sigma l}^n \gamma_n - \sigma v_{\mathbf{k}\sigma l}^n \gamma_n^\dagger)$ [34,38]. Following the standard Bardeen-Cooper-Schrieffer (BCS) approach, the ground state is constructed as a vacuum of Bogoliubov quasiparticles.

The mean-field variables, $\Delta_{0,1}$ and $\Delta_{x/y,1}^\pm$, are calculated self-consistently with convergence criterion set to 10^{-5} [38]. The standard SC OPs are defined in terms of the converged parameters as

$$\begin{aligned}
\Delta_s^l &= \Delta_{0,l} \\
\Delta_{d/s^*}^l &= [(\Delta_{x,l}^+ + \Delta_{x,l}^-) \mp (\Delta_{y,l}^+ + \Delta_{y,l}^-)]/4 \\
\Delta_{px/y}^l &= [\Delta_{x/y,l}^+ - \Delta_{x/y,l}^-]/2. \quad (5)
\end{aligned}$$

The s -, s^* -, p -, and d -wave OPs defined above have their usual meaning as can be verified from the \mathbf{k} dependence of $\Delta_1^{\uparrow\downarrow}(\mathbf{k})$ in limiting cases [33].

IV. TUNNELING-DRIVEN TRANSITIONS

We begin by presenting in Fig. 1 the effect of interlayer hopping \tilde{t} on the SC OPs. We select model parameters such that in the decoupled limit, $\tilde{t} = 0$, different OP symmetries are realized in the SC layer [33]. In Fig. 1(a), we begin with a d -wave OP in the SC layer. For an arbitrarily small value of interlayer hopping, the d -wave OP is induced in the second layer. Near $\tilde{t} = 0.8$, a p -wave component appears in the solution for both the layers. At $\tilde{t} = 1$, the d -wave OP vanishes and the stable solution acquires the $p_x + ip_y$ form. Note that the $p_x + ip_y$ form of the gap function implies that time reversal symmetry is spontaneously broken [39]. Indeed, we have checked that $p_x - ip_y$ is energetically equivalent choice for the symmetry of the order parameter. This is in contrast to the existing proposals for realizing p -wave order wherein strong spin-orbit coupling and an explicit breaking of time reversal is required [24–26]. This unconventional OP reduces gradually on increasing \tilde{t} , and near $\tilde{t} = 2.2$ another transition to an extended s -wave, s^* , form occurs. Therefore, allowing for broken symmetry phases at the mean-field level, we find multiple transitions tuned by interlayer hopping. These transitions are mirrored in the second layer via the proximity effect [see insets in Figs. 1(a)–1(d)]. Eventually, beyond a critical value of the interlayer hopping superconduc-

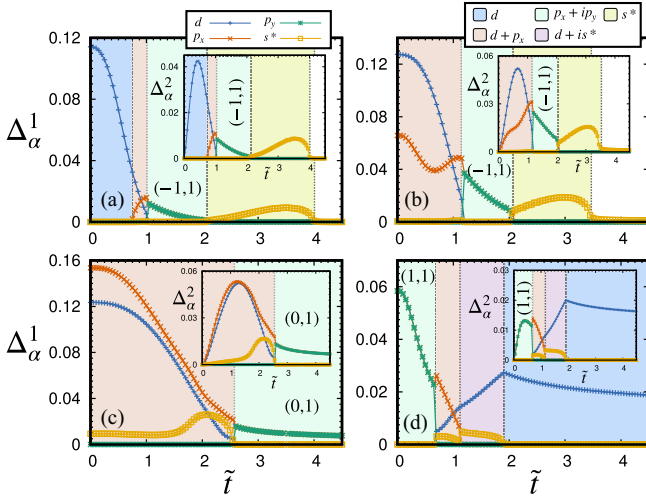


FIG. 1. [(a)–(d)] The self-consistent values of various OPs as a function of interlayer hopping \tilde{t} for $U = 1$ and $t_2 = 1$. Insets show the OP variations in the proximity layer. Different background shades correspond to qualitatively different OP symmetries as indicated. The choice of other parameters is (a) $V = 1.8$, $(n_1 + n_2) = 2.0$; (b) $V = 2.5$, $(n_1 + n_2) = 1.8$; (c) $V = 3.5$, $(n_1 + n_2) = 1.4$; and (d) $V = 2.2$, $(n_1 + n_2) = 0.9$. Integer pairs denote the Chern indices for the two bands wherever at least one is nonzero.

tivity ceases to exist in both the layers in agreement with the previous report on proximity effect [40].

In Fig. 1(b) we demonstrate the occurrence of these transitions starting with a $d + p_x$ -wave OP in the SC layer. The sequence of change in OP symmetries is $d + p_x$ to $p_x + ip_y$ to extended s . The sequence of transitions can be reversed if we begin with a $d + p_x + s^*$ or $p_x + ip_y$ state, as shown in Figs. 1(c) and 1(d). We find that some of these transitions are associated with Lifshitz transitions tuned by \tilde{t} in the noninteracting Hamiltonian [38,41–44]. Note that the $p_x + ip_y$ form of the OP can lead to different band topology depending on the other model parameters [compare Chern indices in Figs. 1(a) and 1(c)].

In these calculations we have kept $\mu_2 = \mu_1$ and the densities in the two layers are allowed to be different. We also perform calculations enforcing equal density in the two layers, which generally requires $\mu_2 \neq \mu_1$. The results are qualitatively identical to those discussed in Fig. 1 [38].

V. CHARACTERIZING THE TOPOLOGICALLY NONTRIVIAL PHASES

We follow two standard approaches to characterize the nontrivial SC states. The first approach involves analyzing Berry curvature and computing topological invariants, known as Chern numbers, associated with each quasiparticle band. We employ an efficient method to calculate Chern numbers, in the discrete Brillouin zone, by making use of $U(1)$ link variable [45],

$$U_n^{\hat{\epsilon}}(\mathbf{k}) = \frac{\langle n(\mathbf{k}) | n(\mathbf{k} + \hat{\epsilon}) \rangle}{|\langle n(\mathbf{k}) | n(\mathbf{k} + \hat{\epsilon}) \rangle|}. \quad (6)$$

In the above, $\hat{\epsilon}$ is a vector connecting nearest neighbor points in the discrete Brillouin zone. The Berry curvature,

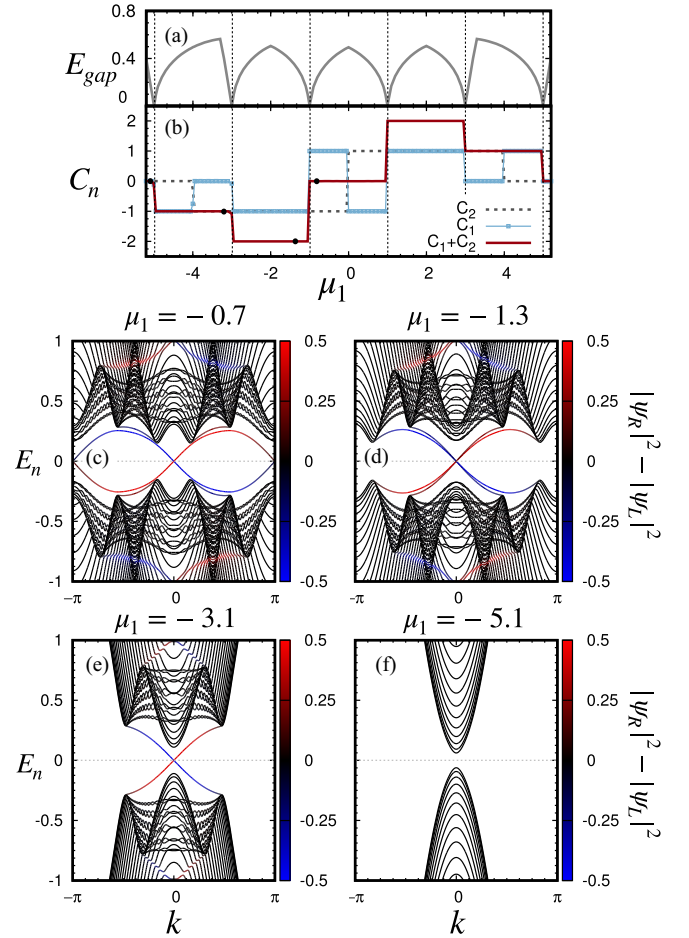


FIG. 2. (a) Variation of the SC gap with chemical potential for $p_x + ip_y$ state. (b) Chern numbers for each band and total Chern index for the same state as in (a). Note that every jump in total Chern index coincides with a closing and reopening of the SC gap. [(c)–(f)] Edge state spectrum in the cylinder geometry for different values of $\mu_1 = \mu_2$. We keep $t_2 = \tilde{t} = 1$ for all the results shown here.

which is gauge invariant, can be calculated as the total phase along a closed loop as

$$F_n(\mathbf{k}) = \frac{1}{i} \ln U_n^{\hat{x}}(\mathbf{k}) U_n^{\hat{y}}(\mathbf{k} + \hat{x}) U_n^{-\hat{x}}(\mathbf{k} + \hat{x} + \hat{y}) U_n^{-\hat{y}}(\mathbf{k} + \hat{y}). \quad (7)$$

Note that the Berry curvature is defined within the principle branch of the logarithm, $-\pi < F_n(\mathbf{k}) \leq \pi$. Summing it over the Brillouin zone gives $2\pi C_n$, where C_n is the Chern number for the n th band.

To illustrate how the topological character of a SC state changes, we select the $p_x + ip_y$ form of the OP. In Fig. 2(a), we show the SC gap as a function of chemical potential. The gap closes and reopens on varying μ_1 . Each such gap closing is associated with a change in the topological character of the bands. This is evident from Fig. 2(b), where we show band-specific as well as total Chern numbers.

The second approach is to compute the edge-state spectra by imposing open boundary conditions in one of the directions, leading to cylinder geometry, and plotting the tower of states as a function of k_x or k_y . Note that only one of k_x and

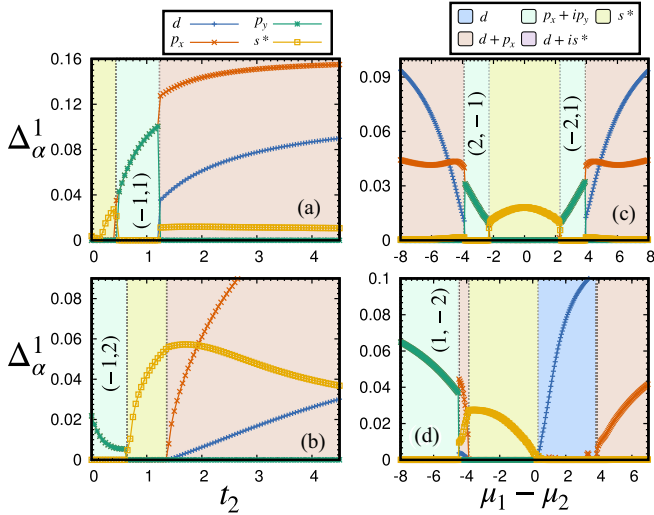


FIG. 3. [(a) and (b)] The values of various OPs as a function of metallic layer hopping t_2 for (a) $\tilde{t} = 1.5$, $(n_1 + n_2) = 1.8$, $V = 4$ and (b) $\tilde{t} = 2.5$, $(n_1 + n_2) = 1.6$, $V = 4$. [(c) and (d)] Variations in the OPs with the gate potential $\mu_1 - \mu_2$ for (c) $t_2 = 1.0$, $\tilde{t} = 2.6$, $\mu_1 = 0$, $V = 2.5$ and (d) $t_2 = 1.0$, $\tilde{t} = 2.25$, $\mu_1 = -1$, $V = 2.5$. Integer pairs denote the Chern indices for the two bands wherever at least one is nonzero.

k_y is a good quantum number in the cylinder geometry. The edge-state spectra are shown in Figs. 2(c)–2(f) for representative values of μ . The color code on the energy eigenvalues represents the difference of the weight on left and that on right edges of the corresponding state. Figure 2(c) shows a case where two states cross the bulk gap; however, the gap is crossed twice. Although both bands have a nonzero (± 1) Chern index, the total Chern index is zero. For $\mu = -1.1$, gap opens close to the Brillouin zone boundary and both the edge states cross the gap only once. In this case the Chern numbers for the two bands add up leading to a total Chern number of -2 . For $\mu = -3.1$, one of the bands pulls away and only one pair of edge states remain. The corresponding Chern number for one of the bands becomes zero, leading to a total Chern number of -1 .

Interestingly, these transitions can also be viewed as Lifshitz transitions in the emergent one-dimensional metallic system residing on the edges in the cylinder geometry. The Fermi surface of this one-dimensional metallic system consists of discrete points. Each instance of change in total Chern number is accompanied by disappearance of a point from the zero dimensional Fermi surface, which can be viewed as a Lifshitz transition in one lower dimension.

VI. TUNING THE TRANSITIONS BY BANDWIDTH AND GATE VOLTAGE

Having shown the existence of unconventional phases in the bilayer model, we ask whether one can tune the system across these transitions by using experimentally viable control parameters. To this end we present the effect of change in bandwidth of the metallic layer and that of gate potential on

SC OPs. In Fig. 3(a), we show the change in various OPs as a function of intralayer hopping t_2 . Taking $t_2 = 1$ as a reference point, we find that a $p_x + ip_y$ state can be tuned to s^* -wave ($d + p_x + s^*$ -wave) state by decreasing (increasing) the bare bandwidth. The sequence of transitions can be altered, as we saw in case of transitions tuned by \tilde{t} , by selecting a different starting point [see Fig. 3(b)]. From an experimental viewpoint the most easily tunable parameter in a possible realization of this model is the difference between on-site potentials in the two layers. We show that the nontrivial transitions in terms of OP symmetries discussed above can also be tuned with the help of parameter $\mu_1 - \mu_2$. Recall that $\mu_1 - \mu_2$ originates from a combination of the on-site energy difference and applied electric field. Two representative cases are shown in Figs. 3(c) and 3(d).

A comment regarding the symmetry aspects of the SC solutions is in order. The various unusual SC states reported here are an outcome of a broken symmetry mean-field analysis. The stability of these phases is controlled by energetics, which relies crucially on the presence of two bands. The mixed symmetry phases, such as $d + p_x$, are examples of spontaneous breaking of parity symmetry, an unusual effect that has recently been observed in experiments [46–50]. In a realistic scenario, presence of additional symmetry breaking terms, such as Rashba coupling, is expected to further stabilize the unusual mixed symmetry states reported here [51].

VII. CONCLUSION

We have shown that a prototype model of proximity-induced superconductivity displays transitions between topologically trivial and nontrivial SC states. Our results are directly relevant to systems that exhibit superconductivity in atomically thin layers, such as monolayer of CuO_2 [28], bilayer graphene [30], NbAs_2 [31], etc. In our calculations, the topological transitions are present for moderate to strong values of attractive Hubbard parameters. Therefore, superconductors that are on the Bose-Einstein condensate (BEC) side of the BCS-BEC crossover are likely to host such effects. The temperatures at which such novel states can be realized in bilayer set-up will certainly be lower than the transition temperatures of SC layer. Furthermore, the bilayer aspect of the model can also be realized in multiorbital systems. Therefore, multiorbital superconductors $\text{Fe}_{1+y}\text{Se}_{1+x}\text{Te}_{1-x}$, which allow for a tuning across the BCS-BEC crossover, are possible candidates [52,53]. Recent spin- and angle-resolved photoemission spectroscopy experiments on $\text{FeSe}_{1-x}\text{Te}_x$ and $\text{LiFe}_{1-x}\text{Co}_x\text{As}$ are suggestive of multiple topological states in these materials [54,55]. Our predictions can also be tested using ultracold Fermions on optical lattices where the interaction strength can be tuned with the help of Feshbach resonances [56–59].

ACKNOWLEDGMENT

We acknowledge the use of High Performance Computing Facility at IISER Mohali.

- [1] J. Kruthoff, J. de Boer, J. van Wezel, C. L. Kane, and R.-J. Slager, *Phys. Rev. X* **7**, 041069 (2017).
- [2] C. L. Kane and E. J. Mele, *Phys. Rev. Lett.* **95**, 226801 (2005).
- [3] C. L. Kane and E. J. Mele, *Phys. Rev. Lett.* **95**, 146802 (2005).
- [4] M. Z. Hasan and C. L. Kane, *Rev. Mod. Phys.* **82**, 3045 (2010).
- [5] J. E. Moore, *Nature* **464**, 194 (2010).
- [6] Y. Cao, V. Fatemi, S. Fang, K. Watanabe, T. Taniguchi, E. Kaxiras, and P. Jarillo-Herrero, *Nature* **556**, 43 (2018).
- [7] F. Wu, A. H. MacDonald, and I. Martin, *Phys. Rev. Lett.* **121**, 257001 (2018).
- [8] L. Aggarwal, A. Gaurav, G. S. Thakur, Z. Haque, A. K. Ganguli, and G. Sheet, *Nat. Mater.* **15**, 32 (2016).
- [9] H. Wang, H. Wang, H. Liu, H. Lu, W. Yang, S. Jia, X.-J. Liu, X. C. Xie, J. Wei, and J. Wang, *Nat. Mater.* **15**, 38 (2016).
- [10] X.-L. Qi and S.-C. Zhang, *Rev. Mod. Phys.* **83**, 1057 (2011).
- [11] A. Bansil, H. Lin, and T. Das, *Rev. Mod. Phys.* **88**, 021004 (2016).
- [12] M. Sato and Y. Ando, *Rep. Prog. Phys.* **80**, 076501 (2017).
- [13] C. Kallin and J. Berlinsky, *Rep. Prog. Phys.* **79**, 054502 (2016).
- [14] L. Fu and C. L. Kane, *Phys. Rev. Lett.* **100**, 096407 (2008).
- [15] C. Nayak, S. H. Simon, A. Stern, M. Freedman, and S. Das Sarma, *Rev. Mod. Phys.* **80**, 1083 (2008).
- [16] A. C. Potter and P. A. Lee, *Phys. Rev. B* **83**, 184520 (2011).
- [17] C. Beenakker, *Annu. Rev. Condens. Matter Phys.* **4**, 113 (2013).
- [18] S. Nadj-Perge, I. K. Drozdov, J. Li, H. Chen, S. Jeon, J. Seo, A. H. MacDonald, B. A. Bernevig, and A. Yazdani, *Science* **346**, 602 (2014).
- [19] M. Ruby, F. Pientka, Y. Peng, F. Von Oppen, B. W. Heinrich, and K. J. Franke, *Phys. Rev. Lett.* **115**, 197204 (2015).
- [20] C. Beenakker and L. Kouwenhoven, *Nat. Phys.* **12**, 618 (2016).
- [21] V. Mourik, K. Zuo, S. M. Frolov, S. R. Plissard, E. P. A. M. Bakkers, and L. P. Kouwenhoven, *Science* **336**, 1003 (2012).
- [22] L. P. Rokhinson, X. Liu, and J. K. Furdyna, *Nat. Phys.* **8**, 795 (2012).
- [23] R. Pawlak, M. Kisiel, J. Klinovaja, T. Meier, S. Kawai, T. Glatzel, D. Loss, and E. Meyer, *npj Quantum Inf.* **2**, 16035 (2016).
- [24] J. Wiedenmann, E. Bocquillon, R. S. Deacon, S. Hartinger, O. Herrmann, T. M. Klapwijk, L. Maier, C. Ames, C. Brüne, C. Gould, A. Oiwa, K. Ishibashi, S. Tarucha, H. Buhmann, and L. W. Molenkamp, *Nat. Commun.* **7**, 10303 (2016).
- [25] C. Li, J. C. de Boer, B. de Ronde, S. V. Ramankutty, E. van Heumen, Y. Huang, A. de Visser, A. A. Golubov, M. S. Golden, and A. Brinkman, *Nat. Mater.* **17**, 875 (2018).
- [26] Y. Volpez, D. Loss, and J. Klinovaja, *Phys. Rev. B* **97**, 195421 (2018).
- [27] T. Zhang, P. Cheng, W.-J. Li, Y.-J. Sun, G. Wang, X.-G. Zhu, K. He, L. Wang, X. Ma, X. Chen, Y. Wang, Y. Liu, H.-Q. Lin, J.-F. Jia, and Q.-K. Xue, *Nat. Phys.* **6**, 104 (2010).
- [28] G.-Y. Zhu, F.-C. Zhang, and G.-M. Zhang, *Phys. Rev. B* **94**, 174501 (2016).
- [29] M. S. Scheurer and J. Schmalian, *Nat. Commun.* **6**, 6005 (2015).
- [30] A. M. Alsharari, M. M. Asmar, and S. E. Ulloa, *Phys. Rev. B* **97**, 241104(R) (2018).
- [31] Y. Li, C. An, C. Hua, X. Chen, Y. Zhou, Y. Zhou, R. Zhang, C. Park, Z. Wang, Y. Lu, Y. Zheng, Z. Yang, and Z.-A. Xu, *npj Quantum Mater.* **3**, 58 (2018).
- [32] A. V. Suslov, A. B. Davydov, L. N. Oveshnikov, L. A. Morgun, K. I. Kugel, V. S. Zakhvalinskii, E. A. Pilyuk, A. V. Kochura, A. P. Kuzmenko, V. M. Pudalov, and B. A. Aronzon, *Phys. Rev. B* **99**, 094512 (2018).
- [33] S. Nayak and S. Kumar, *J. Phys.: Condens. Matter* **30**, 135601 (2018).
- [34] P.-G. DeGennes, *Superconductivity of Metals and Alloys* (Advanced Book Program, Perseus Books, Cambridge, MA, 1999).
- [35] Jian-Xin Zhu, *Bogoliubov-de Gennes Method and Its Applications* (Springer International Publishing, Cham, 2016).
- [36] M. Sigrist and K. Ueda, *Rev. Mod. Phys.* **63**, 239 (1991).
- [37] S. Diesch, P. Machon, M. Wolz, C. Sürgers, D. Beckmann, W. Belzig, and E. Scheer, *Nat. Commun.* **9**, 5248 (2018).
- [38] See Supplemental Material at <http://link.aps.org/supplemental/10.1103/PhysRevB.100.214517> for further details.
- [39] A. P. Mackenzie and Y. Maeno, *Rev. Mod. Phys.* **75**, 657 (2003).
- [40] A. Zujev, R. T. Scalettar, G. G. Batrouni, and P. Sengupta, *New J. Phys.* **16**, 013004 (2014).
- [41] G. E. Volovik, *Low Temp. Phys.* **43**, 47 (2017).
- [42] K.-S. Chen, Z. Y. Meng, T. Pruschke, J. Moreno, and M. Jarrell, *Phys. Rev. B* **86**, 165136 (2012).
- [43] J. Lin, *Phys. Rev. B* **82**, 195110 (2010).
- [44] Y. Shi, S. Che, K. Zhou, S. Ge, Z. Pi, T. Espiritu, T. Taniguchi, K. Watanabe, Y. Barlas, R. Lake, and C. N. Lau, *Phys. Rev. Lett.* **120**, 096802 (2018).
- [45] T. Fukui, Y. Hatsugai, and H. Suzuki, *J. Phys. Soc. Jpn.* **74**, 1674 (2005).
- [46] A. Trenkwalder, G. Spagnolli, G. Semeghini, S. Coop, M. Landini, P. Castilho, L. Pezzè, G. Modugno, M. Inguscio, A. Smerzi, and M. Fattori, *Nat. Phys.* **12**, 826 (2016).
- [47] G. J. Shu and F. C. Chou, [arXiv:1212.6647](https://arxiv.org/abs/1212.6647).
- [48] F. Giacosa, *Eur. Phys. J. C* **65**, 449 (2010).
- [49] I. A. Sergienko, *Phys. Rev. B* **69**, 174502 (2004).
- [50] N. Read and D. Green, *Phys. Rev. B* **61**, 10267 (2000).
- [51] T.-P. Choy, J. M. Edge, A. R. Akhmerov, and C. W. J. Beenakker, *Phys. Rev. B* **84**, 195442 (2011).
- [52] Y. Lubashevsky, E. Lahoud, K. Chashka, D. Podolsky, and A. Kanigel, *Nat. Phys.* **8**, 309 (2012).
- [53] S. Rinott, K. B. Chashka, A. Ribak, E. D. L. Rienks, A. Taleb-Ibrahimi, P. Le Fevre, F. Bertran, M. Randeria, and A. Kanigel, *Sci. Adv.* **3**, e1602372 (2017).
- [54] P. Zhang, K. Yaji, T. Hashimoto, Y. Ota, T. Kondo, K. Okazaki, Z. Wang, J. Wen, G. D. Gu, H. Ding, and S. Shin, *Science* **360**, 182 (2018).
- [55] P. Zhang, Z. Wang, X. Wu, K. Yaji, Y. Ishida, Y. Kohama, G. Dai, Y. Sun, C. Bareille, K. Kuroda, T. Kondo, K. Okazaki, K. Kindo, X. Wang, C. Jin, J. Hu, R. Thomale, K. Sumida, S. Wu, K. Miyamoto, T. Okuda, H. Ding, G. D. Gu, T. Tamegai, T. Kawakami, M. Sato, and S. Shin, *Nat. Phys.* **15**, 41 (2019).
- [56] J. T. Stewart, J. P. Gaebler, and D. S. Jin, *Nature* **454**, 744 (2008).
- [57] C. Chin, M. Bartenstein, A. Altmeyer, S. Riedl, S. Jochim, J. H. Denschlag, and R. Grimm, *Science* **305**, 1128 (2004).
- [58] G. B. Partridge, K. E. Strecker, R. I. Kamar, M. W. Jack, and R. G. Hulet, *Phys. Rev. Lett.* **95**, 020404 (2005).
- [59] T. Graß, R. W. Chhajlany, L. Tarruell, V. Pellegrini, and M. Lewenstein, *2D Mater.* **4**, 015039 (2016).